REFLECTANCE SPECTROSCOPY IN GEOLOGY AND SOIL SCIENCES: LITERATURE REVIEW

Ireneusz Badura , Maciej Dąbski

Department of Geomorphology, Faculty of Geography and Regional Studies, University of Warsaw, Poland

Manuscript received: May 31, 2022
Revised version: August 3, 2022

Badura I., Dąbski M., 2022. Reflectance spectroscopy in geology and soil sciences: Literature review. *Quaestiones Geographicae* 41(3), Bogucki Wydawnictwo Naukowe, Poznań, pp. 157–167. 3 figs, 1 table.

Abstract: This article presents a literature review of studies utilising reflectance spectroscopy in geological research. We describe a variety of available spectral libraries together with providing examples of spectral reflectance diagrams, and explain the basic spectral ranges. Geologists can use different methods of data collection, for example, sensors mounted on satellites, airborne [including unmanned aerial vehicle (UAV) platforms] or portable spectroradiometers, and different ways of data processing. Most geological mapping based on reflectance spectroscopy is performed in the Arctic region, where vegetation does not obscure images. However, mineral mapping, studies of hot spring deposits, and rock/soil weathering alterations are also performed in lower latitudes. The development, combination and unification of all spectral data acquisition methods open up new possibilities for applications in a variety of geological and soil studies.

Key words: reflectance spectroscopy, mineral spectra, geological mapping, soil studies

Corresponding author: Maciej Dąbski; mfdabski@uw.edu.pl

Introduction

Spectroscopy is the precise study of a spectrum of electromagnetic radiation that has been emitted, reflected or scattered from any type of surface. There are a variety of spectroscopic techniques using different types of radiation with different ways of interaction with rocks or soils. This allows obtaining a variety of information on the atomic, ion or mineral composition of the study surfaces. Spectral measurement devices are referred to as spectrometers, spectrophotometers, spectrographs or spectral analysers, and are widely used in many fields of Earth sciences, usually in association with remote sensing (e.g. sensors mounted on satellites or airplanes). However, this method seems to be relatively neglected in geological research (*sensu largo*) or soil studies in many parts of the world. Spectroscopic information about the mineral content of the ground, whether soft sediment, regolith or hard rock, constitutes a great tool in numerous geological, geomorphological and soil studies. It includes mapping of rocks and mineral outcrops, assessment of rock weathering degree, soil studies, analysis of minerals, protection of the natural environment, analyses of geothermal deposits and studies of meteorites. This article aims to present a literature review of the use of reflectance spectroscopy, which focuses on light wavelengths that have been reflected by hard rocks, sediments, regolith or soils

https://doi.org/10.2478/quageo-2022-0031
ISSN 2082-2103, eISSN 2081-6383

(Kortüm 1969) in geological and soil studies and to highlight the most important current study directions in this field. Our review does not aim to encompass studies dealing with the full range of spectrometric techniques, including RAMAN, atomic absorption, X-ray, gas chromatography, optical emission, and gamma-ray spectroscopy, but rather to focus on those studies dealing with the most popular spectrometric technique deployed in Earth sciences and remote sensing, namely reflectance spectroscopy, which has not yet been fully studied by researchers.

Beginnings, spectral libraries and manuals

The study of electromagnetic wavelength absorption or reflectance by minerals, soils or solid rock surfaces has been intensively used in geology since the 1970s, when significant developments in this matter were published by Hunt (1970), Hunt and Salisbury (1971) and Hunt et al. (1971a, b, 1972, 1973), to be finally summarised by Hunt (1977). The works mentioned provided the first comprehensive sets of visible and near-infrared (VNIR) spectra of minerals and rocks. The advantages of spectroscopy in geological studies, based on aircraft and satellites, as a technically feasible method, were highlighted by Goetz et al. (1985). This marked the onset of a remarkable development in geological remote sensing. Clark et al. (1990) emphasised the need for focusing on the spectral range between 0.4 μm and 2.5 μm in the deployment of VNIR and shortwave-infrared (SWIR) because it contains the most important spectral features of hydroxyl-bearing minerals, sulphates and carbonates common to many geologic units.

Nowadays, collections of thousands of spectral reflectance curves are assembled in spectral libraries to facilitate laboratory observations, field spectroscopy and remote sensing for identifying and mapping various surface units in relation to the Earth. For the recognition of minerals or rocks, several reference databases have been created in mineral spectral libraries, as well as for the analysis and matching of unknown features (Mulder et al. 2013). Mineral or rock spectral data (Fig. 1) are stored in different spectral libraries worldwide (e.g. Grove et al. 1992, Clark et al. 1993, Tong et al. 1998, Kokaly et al. 2017), which unfortunately, has resulted in differences in various experimental parameters, such as measurement conditions, particle size and geodesic structures (Li 2008). Xie et al. (2020) undertook a trial to design and develop an integrated mineral spectral library collected from the shared data worldwide with special software (Table 1).

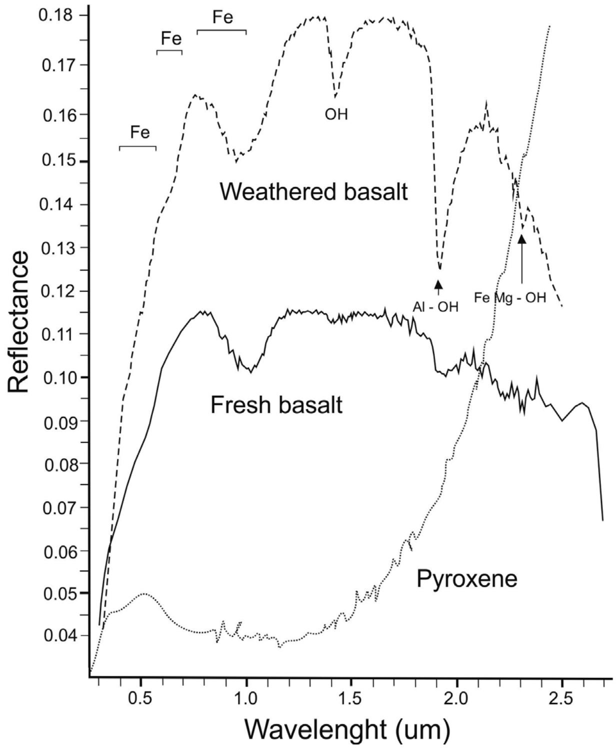

Fig. 1. Examples of spectral reflectance diagrams for fresh and weathered basaltic rocks and pyroxene (based on Kokaly et al. 2017, Zhou and Wang 2017, modified). Selected spectral features are marked acc. to Zhou and Wang (2017).

Version 2 of the Advanced Spaceborne Thermal Emission and Reflection Radiometer (ASTER) Spectral Library includes additions to the mineral and rock spectra and provides one of the most comprehensive collections of spectra available for geologists, geomorphologists and soil scientists (Baldridge et al. 2009). However, the use of different spectral resolutions in different libraries, different mineral categories and measurement parameters can still impede their application in field investigation, mineral identification, land cover classification and geological mapping.

Principles of spectroscopy of rocks and minerals are described in the manuals relating to spectral libraries, such as the United State Geological

Table 1. A selection of current widely available spectral libraries (based on Xie et al. 2020, modified).

Release year	Spectral library	Institution
1978	Infrared spectrogram database	Shanghai institute of organic chemistry, Chinese Academy of Sciences
1981	JPL spectral library	Jet propulsion laboratory JPL, California Institute of Technology
1990	ICGP-264 spectral library	United States Geological Survey USGS
1990	Ground object reflectance spectral characteristics database	Institute of optical machinery, Chinese Academy of Sciences
1991	JHU spectral library	Johns Hopkins University JHU
1993	USGS spectral library	United States Geological Survey USGS
1998, 2008	ASTER spectral library (version 1 and 2)	America's space agency, NASA
2000	ASU Thermal infrared spectrum library	Arizona State University ASU
2002	China typical feature spectrum library	Beijing Normal University
2007	National typical ground object spectrum database for e-government	Institute of Remote Sensing Earth, Chinese Academy of Sciences

Survey user's manual for program SPECPR (Clark 1993, 1999). To understand spectroscopy, one needs to understand some basic terms such as spectral range, spectral bandwidth, spectral resolution and sampling and signal-to-noise ratio (S/N). The spectral range is the range of wavelengths that each spectrometer can measure. Several ranges can be distinguished:

a) ultraviolet (UV): 0.1–0.4 μm,
b) visible radiation: 0.38–0.76 μm,
c) near-infrared (NIR): 0.75–1.4 μm,
d) short wavelength infrared (SWIR): 1.4–3 μm,
e) mid-wavelength infrared (MWIR): 3–8 μm,
f) long-wavelength infrared (LWIR): 8–15 μm, and
g) far-infrared (FIR): 15–1000 μm.

Ranges covering wavelengths of 0.75–15 μm (NIR + SWIR + MWIR + LWIR) are called thermal infrared (TIR) due to the properties of non-contact temperature measurements. The visible and NIR radiation range together are called visible near-infrared (VNIR), and this has been mostly used in geological and soil studies. The spectral bandwidth informs about the width of a specific reflectance maximum. Spectral sampling resolution is the maximum separating or discriminating power of measurement, and spectral frequency informs the frequency of the data collection. The S/N compares the level of the desired signal with the level of background noise (unwanted fluctuation in a signal).

Hyperspectral data processing of satellite or aerial images requires extraction of endmembers, which are diagnostic signatures used to specify a spectral class. Different algorithms of endmember extraction (e.g. linear unmixing model) and image classification techniques are described in suitable detail by Peyghambari and Zhang (2021).

Spectrometry in geological mapping

The beginnings of the application of spectrometry for mineral mapping took place in the 1970s with the use of aerial scanning in Nevada (Abrams et al. 1977). The Airborne Imaging Spectrometer (AIS) provided, for the first time, the possibility of obtaining mineralogical maps of the Earth's surface (Goetz, Srivastava 1985). The development of the first spectral libraries and algorithm methods automated and facilitated the mapping of minerals (Kruse, Lefkoff 1994). Later, the ASTER sensor aboard the Earth Observing System (EOS) Terra satellite launched in 2000 provided revolutionary new capabilities for cost-effective mineral and land cover mapping over large areas. The ASTER sensor acquires multispectral data in 14 bands, including 4 bands in VNIR (0.52–0.86 μm), 5 bands in the SWIR (1.6–2.43 μm) and 5 bands in TIR (thermal region (8125–11.65 μm).

Hellman and Ramsey (2004) used the ASTER and Airborne Visible/IR Image Spectrometer (AVIRIS) data to characterise hot spring deposits in Yellowstone National Park. Using images based on VNIR and TIR radiation, they were able to locate areas of thermal alteration, an abundance of alteration minerals and a comparison of active, near-extinct and extinct geysers. This study proved that spectroscopy can be used in studies of extinct mineralised hydrothermal deposits on both Earth and Mars. As proven by Rockwell and Hofstra (2008), the TIR data of ASTER are vital for detecting non-hydrous varieties of quartz that are not spectrally identifiable in the visible, near-infrared and shortwave-infrared (SWIR) spectral regions owing to a lack of diagnostic absorption features. In Kumar et al. (2020), another example has been provided of the use of the ASTER library in accompaniment with an airborne spectrometer (AVRIS-NG), where the researchers proposed an automated lithological mapping of the gold-bearing granite-greenstone belt of Hutti area.

Mapping gold deposits or other hydrothermal alteration of rocks using ASTER and/or Landsat sensors has become very common in Africa in recent years (Traore et al. 2020, Andongma et al. 2021, El-Desoky et al. 2022).

Salehi et al. (2019) compared two different multispectral datasets obtained from (1) ASTER and (2) Sentinel-2, during the mapping of geological units in NE Greenland. The study outcomes proved that ASTER data are more suitable for discriminating between various lithological units, owing to the reasons that: (1) ASTER has six SWIR bands in comparison with just two bands offered by Sentinel-2 and (2) Sentinel-2 does not contain TIR bands. However, the latter Sentinel-2 provided better data for the detection of iron-bearing minerals due to several bands covering the 0.9 μm iron absorption feature (much more than ASTER).

There are different methods of spectral data processing. Rogge et al. (2007) used the spatial-spectral endmember extraction tool (SSEE), which works by analyzing a scene in parts (subsets), and allows increasing the spectral contrast of low-contrast rock endmembers. The study was performed on images obtained over Nevada and Baffin Island and showed that the SSEE method was an effective approach for extracting endmembers.

In SW Greenland, lithologies were mapped by Bedini et al. (2009) with use of the HyMAP airborne hyperspectral imaging system and unsupervised clustering algorithm, the Self Organising Maps (SOM) and a hierarchical tree. The resulting lithological map showed the spatial distribution of dolomite carbonatite, søvite, fenite with abundant carbonatite dykes, and fenite and hematised gneiss (marginal alteration zone).

Field data collection proved that the map based on spectral data was accurate and suitable for the mapping of carbonatite lithologies. HyMAP images, obtained over the Spanish Gabo de Gata volcanic area, were also used by van der Meer et al. (2018). The study proved that Wavelength Mapper and QuanTools are algorithms that can be effectively used to produce consistent, comparable and reproducible maps.

Identification of spectral indices that can directly reflect the ratio of the rock and lichen in hyperspectral data was a focus of studies performed in Greenland by Salehi et al. (2016, 2017, 2020) and Salehi (2018). By analysing HyMAP images, they investigated how lichen cover affects the characteristics of SWIR mineral absorption

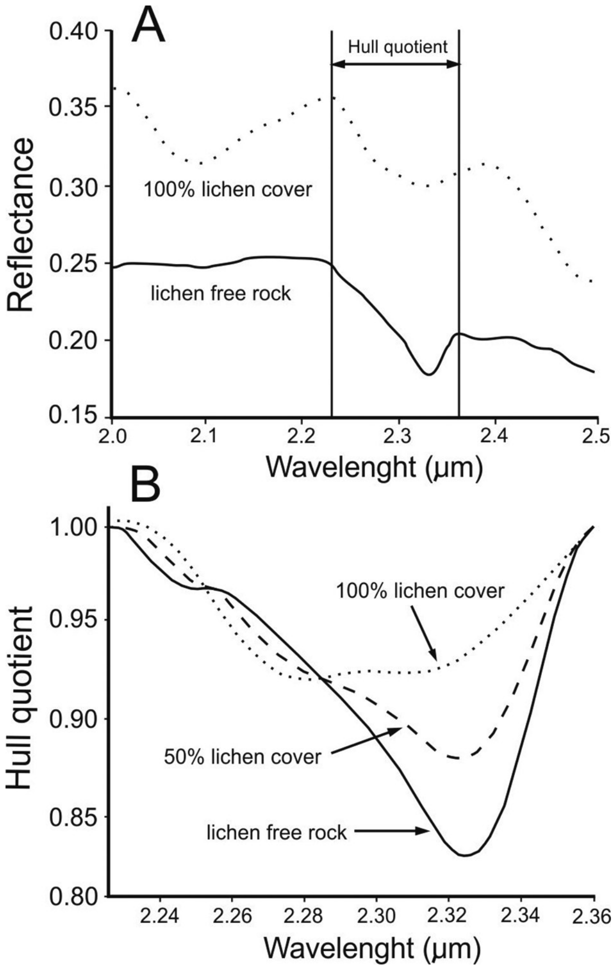

Fig. 2. A – Averaged spectra of kimberlite rock with and without crustose lichen cover, B – The corresponding hull quotient (Clark, Roush 1984) with spectra associated with the antigorite absorption feature (acc. to Salehi et al. 2017, modified).

features and developed an automated absorption feature extraction algorithm. Figure 2 shows the obtained wavelength displacement of characteristic absorption features for a kimberlite rock with different percentages of crustose lichen cover. The studies of the above-mentioned authors emphasise the importance of a careful selection of wavelengths for image analysis in environments where bedrock is significantly overgrown with lichens, which is a common situation in the subpolar and polar zones.

The study of Pal et al. (2020) can be mentioned as an example of lithological classification using several multi- and hyperspectral space-borne sensors. They used VNIR and SWIR bands of Hyperion, ASTER and Landsat 8 images. In a study of the Udaipur area (India), they successfully discriminated different sedimentary and metamorphic lithoclasses, including quartzite, phyllite, graywacke, dolomite, mafic-metavolcanics, migmatite, graphitic metapelites and quartzite-arkose-conglomerate.

Major lithologies of the Karkonosze Mountains (Poland) were studied in-field with the use of the ASD FieldSpec spectrometer and images were obtained from VITO's Airborne Prism EXperiment (APEX) scanner (Mierczyk et al. 2016). Bare rock surfaces were difficult to detect due to coverage by lichens or vascular plants. However, hyperspectral airborne imagery allowed for subpixel classifications of different types of granites, hornfels and mica schist after the implementation of advanced algorithms such as Spectral Angle Mapper, Linear Spectral Unmixing and Matched Filtering (the latter being the most effective).

The development of technology in the past decade allows the construction of multispectral sensors for unmanned aerial vehicles (UAVs). The first sensors allowed the mapping of iron-bearing minerals such as hematite, jarosite and goethite that have characteristic spectral features in the visible near-infrared (Gupta 2018). The research scenario in relation to UAV-borne multispectral surveys is progressing quickly and promisingly, and it is largely anticipated that subsequent research would bring forth better and better spectral resolutions (Heinicke et al. 2019). Geological mapping from the UAVs allows for quick data acquisition from small and intermediate areas, bridging the gap between field observations and airborne surveys (Martlet et al. 2021).

Parish (2016) evaluated reflectance spectroscopy as a method of determining chert provenance, and the implications of this research carry significance for forthcoming archaeological research. He analysed 2430 samples from 81 deposits collectively representing seven chert types in the Midwestern and South-eastern United States, and concluded that the combined use of VNIR and Fourier transform infrared (FTIR) reflectance spectroscopy is an accurate and fast method for characterisation of chert deposits. The capability of reflectance spectroscopy to accurately assign a chert source can be of great importance in tracking the movement and behaviour of prehistoric (Stone Age) people.

Spectrometry in rock weathering studies

Reflectance spectroscopy together with colourimetry can be used in the determination of the rock weathering stage. Nagano and Nakashima (1989) used these methods to determine the degree of weathering of powdered granitic rocks in Japan, rightly assuming that an increase in the yellow-brownish FeO(OH) content testifies to a more advanced stage of weathering. This was further supported by Younis et al. (1997), who measured spectral characteristics (VNIR) of sedimentary and igneous rocks (sampled in Spain) with various degrees of weathering. They found that brightness and presence of characteristic absorption features result mainly from the iron oxides that had precipitated during weathering.

Zhang et al. (2007) utilised ASTER images (VNIR and SWIR) showing parts of California to elaborate four rock weathering alteration indices from the six SWIR channels and determined alteration zones using a PCA-transformed mineralogic indices approach. Spectrally mapped flood basalt, quartz-biotite gneiss, muscovite schist and granitic, volcanic and metasedimentary rock units showed very good overlapping with the reference geologic map (the overall classification accuracy was 82%). The constrained energy minimisation technique (a subpixel unmixing algorithm) was used to detect significant alteration minerals such as alunite, kaolinite, muscovite and montmorillonite.

Fig. 3. The spectroradiometer ASD FieldSpec used in weathering studies in front of Hallstätter Glacier in the Alps (photo M. Dąbski).

Variations in rock brightness, presence and intensity of characteristic absorption features, and the spectral slope were detected also by Zhou and Wang (2017), who studied rock samples collected in Xinjiang (China). The mineral composition of the weathered surfaces was determined by a BJKF-II portable NIR mineral analyser (Nanjing Instrument Co. Nanjing, China), and reflectance spectra were measured with the use of a portable spectroradiometer, ASD FieldSpec (Malvern Panalytical Ltd, Malvern, UK).). The spectral resolution was 0.003 μm at band ranges of 0.350–1.0 μm and 0.008 μm at 1.0–2.5 μm. They found that spectral differences between weathered and fresh rock surfaces were small for rhyolite, granite and tuffaceous sandstone, but large for andesite, basalt (Fig. 1) and diorite. Spectral changes in the 0.35–1 μm wavelength region were attributed to weathering of iron-rich minerals. However, the region of 1–2.5 μm shows O–H vibrations, and features at 2.2–2.5 μm can be solely attributed to hydroxyl groups. The strongest Al–OH bands appear near 2.2 μm, while Mg–OH bands were found near 2.3 μm and 2.35 μm.

Park and Kim (2019) successfully used narrow-band multispectral (NBMS) analysis and a spectral index classification algorithm to detect weathered features on rock surfaces on Mt. Lemmon in Arizona. Spectral images were collected from rock slopes using a portable VNIR hyperspectral camera. Wavelength ratios of 0.601–0.550 μm and 0.993–0.450 μm were used to delineate weathered and aperture areas, respectively, on the rock mass. The weathering degree of rocks was then elaborated using thematic images. The percentages of the weathered and aperture areas were used in a modified Geological Strength Index (GSI) evaluation.

Schaefer et al. (2021) presented the use of reflectance spectroscopy to estimate rock properties in the volcanic area of Mt. Ruapehu (New Zealand). They could determine connected porosity, strength, magnetic susceptibility and elasticity using the SWIR parts of the electromagnetic spectrum. They attributed this correlation to the presence or degradation (i.e. weathering or hydrothermal alteration) of iron-bearing minerals such as pyroxene, magnetite and pyrite, which reflect changes to both rock properties and spectral reflectance data.

The authors of this article currently investigate (data in elaboration) rock spectral reflectance in a sequence of test sites running from contemporary glacial margins to Little Ice Age moraines in the Alps and Svalbard using ASD FieldSpec (Fig. 3). They search for reflectance curve characteristics indicative of advancing weathering in different petrographic conditions and different climatic zones (initial results are promising).

From the very beginning of spectroscopic application in Earth sciences, geologists have successfully used this method to study meteorites.

Terrestrial weathering of chondrites (stony meteorites) was researched by Salisbury and Hunt (1974). They found excellent correlation between steepening of slope in the visible radiation and a deepening of the 3 μm band, consistent with a progressively greater abundance of weathering products (hydrate and hydroxyl). Spectral reflectance (VNIR) of a variety of meteorites has been also measured by Gaffey (1976), who grouped meteorites into: (1) those with strong spectral features (ordinary chondrites, basaltic achondrites, diogenites, nakhlites, angrites and chassignites), (2) those with weak features (ureilites, black chondrites, stony-irons and some of the carbonaceous chondrites) (3) and those which are featureless (iron meteorites, enstatite chondrites, achondrites and some of the carbonaceous chondrites). Gaffey (1976) concentrated on unweathered meteorites; however, in one case, he noticed an evident signature of terrestrial wreathing: Alais, a carbonaceous chondrite, exhibited a spectral water-related feature at 1.9 μm, which must have resulted from terrestrially absorbed water.

Spectrometry in soils studies

Hyperspectral and multispectral images (encompassing radiation spectrum from visible radiation to MWIR) constitute the basis for soil studies and precision agriculture. Satellite or airborne remote sensing is increasingly used for proper application of fertilisers, pesticides and irrigation, because this technique provides up-to-date information on soil moisture, type of crop cover and crop health (Liaghat, Balasundram 2010). Reflectance spectroscopy (satellite and aerial imaging, and *in situ* or laboratory measurements) is intensively used in the mapping of a variety of soil characteristics, for example, soil erosion, exhaustion, salinisation and mineral composition.

A comprehensive study was published by de Jong (1994), who used airborne and laboratory VNIR images to delineate areas effaced by or potentially vulnerable to soil degradation by gully erosion in southern France. A multivariate approach, visual interpretation, and convex-hull transformation on the spectral curves were used. However, the spectral images obtained did not correlate well with the pattern derived from classic soil erosion models, and this was attributed to vegetation, which impeded the proper interpretation of spectral data.

Hyperspectral imagery can be effectively used to map a deep weathering front (regolith depth) and different degrees of weathering on granite rock (Riaza et al. 1997). Spectral images provided by airborne spectrometer DAIS 7915 (72 channels in 2.5–4 μm, and 7 in 8–12.5 μm bandwidths) were used to produce maps highlighting areas of significant erosion associated with landforms, topography and climate. Such maps contribute to understanding factors responsible for soil granulometry and soil depth and, consequently, help to elaborate soil loss and soil conservation maps.

Spectral characteristics of wet-sieved soil samples (representing relatively undisturbed soil) were compared with the characteristics of dry-sieved samples (represented disturbed soils) by Johnson et al. (1998). They used a portable μFT-IR field spectrometer that detects 3–5 μm and 7–14 μm bandwidths. The study found that the undisturbed soil samples had greater spectral contrast in the region near 9 μm, probably resulting from the removal of fine-grain coating, mainly kaolinitic clay, upon the action of rain (or snowmelt) water or wind deflation occurring naturally in nature.

Demattê and Garcia (1999) measured spectral reflectances (VNIR) of soil samples collected at 0–0.2 m and 0.4–0.6 m depths with the use of Infra-Red Intelligent Spectroradiometer (IRIS). The soils included arguidolls, rhodudalfs and hapludox developed on basalts in the Paraná state. In general, the deeper soil horizons exhibited higher reflectance intensities than the upper ones. Soil organic matter was responsible for lowering of reflectance intensity in the entire spectrum; however, amorphous and crystalline Fe influenced reflectance differently. Multivariate analysis demonstrated that the content of clay, silt, kaolinite, crystalline Fe, amorphous Fe and Mg can be determined by analysis of the reflected energy of the soils. The study proved that soils can be separated at the soil-type level based on the reflectance intensities in various absorption bands.

Multivariate statistical analysis was applied by Leone and Sommer (2000) to high-resolution laboratory reflectance spectra of soil samples reflecting the range of soil development in the southern Apennines. They found that the brightness and

VNIR slope of the spectra are important spectral characteristics that can be used to discriminate soil development, most importantly carbonate content, organic matter and soil texture. Soil types could be further separated based on the iron oxide features and the two main water and hydroxyl absorption bands at 1.4 μm and 1.9 μm.

VNIR has been used in soil studies to evaluate soil horizons and processes in various soil types (e.g. message, decalcification, dessilication and ferralisation), chronosequences and morphoclimatic zones. Reflectance spectrometry of soil samples can provide quantified information about colour, organic carbon, moisture, exchangeable calcium and magnesium cation (Varshney, Arora 2004). An interesting study was performed by Michalski et al. (2006), who compared fresh and weathered basalts sampled in Washington state (USA) using VNIR and thermal emission (6–30 μm) spectral ranges. They found that weathered basalt surfaces exhibit increased reddening and brightening (observed in VNIR), and increased silica and clay content (observed in thermal IR). Their results can have significant implications for studies of chemical weathering processes on Mars, because spectral images of the Red Planet show variably oxidised surfaces and the presence of amorphous silica and clay-like materials in the TIR.

Selected Brazilian soils (oxisols and ultisols in Goiás state) were mapped together with quantification of their mineralogical components with use of the AVIRIS sensor (VNIR) by Baptista et al. (2011). By applying the spectral index RCGb [kaolinite/(kaolinite + gibbsite) ratio], the authors were able to effectively determine the weathering degree of the soils and the transition between oxisols and ultisols. The detected kaolinite and gibbsite content of the soils was checked against laboratory mineralogical quantification.

Mohanty et al. (2016) demonstrated a new approach to estimating weathering indices in soils in West Bengal and Odisha states (India). VNIR and MIR radiation spectra were used and spectral measurements were made with use of a portable spectroradiometer, ASD FieldSpec (VNIR), and an FTIR spectrometer (Nicolet 6700) for MIR. The robustness of spectral models was checked by the residual prediction deviation (RPD). MIR data provided superior estimation capability for all weathering indices compared with VNIR data. The best prediction was obtained for index of laterisation in the MIR and MgIndex in VNIR. The variable importance projection (VIP) approach produced the best results when both spectral ranges were combined, especially for a chemical index of alteration, mafic index of alteration, index of lateralisation and weathering index of Parker. This study provided further arguments that soils may be estimated in a rapid and non-destructive way *in situ*.

Chemical, physical and mineralogical properties of soil change over time and these trends exhibit rates and directions of pedogenic processes. Zheng et al. (2019) studied a soil chronosequence derived from 1000-year-old calcareous marine sediments in Northern Jiangsu Province with use of a portable spectrometer, ASD FieldSpec. They showed that soil organic matter accumulation, $CaCO_3$ leaching and clay migration can be identified in the millennium chronosequence using the reflectance intensity and absorption features. However, the absorption features of Fe did not exhibit evident changes with age in the studied soil chronosequence.

A similar study, based on soil samples and ASD FieldSpec measurements, was performed by Chang et al. (2020) in order to determine the spatial pattern of soil degradation (mostly salinisation and alkalisation) in the Yellow River Delta. They created a soil degradation index (SDI) using the entropy weight method based on a variety of soil indices (pH, SSC, OM, AN, AP and AK). The overall reflectance spectra increased together with increased level of soil degradation. Correlation between SDI and selected spectral parameters was determined.

Conclusion

Reflectance spectroscopy is a rapidly evolving science that can be used in geology-related applications and soil sciences where other methods are impossible, troublesome or time-consuming. Owing to the availability of open access to established spectral libraries offering spectral diagrams for a wide variety of rocks and minerals, and an abundance of relevant literature, mineralogical and petrographic structures are becoming easily determined at various scales and locations. The method can be used directly in-field (owing to the advent of portable spectrometers), under laboratory conditions (e.g. focusing on rock or soil samples) or by processing and interpreting UAV surveys, airborne or satellite images. The development, combination and unification of all these data sources open up new possibilities for application in a variety of geological studies, including mapping of minerals, rocks of various petrographic composition, soils and weathering alterations.

Acknowledgements

The spectroradiometer ASD FieldSpec used in weathering studies in front of Hallstätter Glacier in the Alps was provided by MGGP Aero. This research was funded wholly by the National Science Centre, Poland (NCN), grant 'Micro-weathering and spectral signatures of rock surfaces in glacier forelands' (2020/39/O/ST10/01068). The authors thank the anonymous reviewers for their valuable comments.

Author's Contribution

All authors contributed equally towards conducting the research, drafting the manuscript, and revising it critically for important intellectual content.

References

Abrams M.J., Ashley R.P., Rowan L.C., Goetz A.F.H., Kahle A.B., 1977. Mapping of hydrothermal alteration in the cuprite mining district, Nevada, using aircraft scanner images for the spectral region 0.46 to 2.36 μm. *Geology* 5(12): 713–718.

Andongma W.T., Gajere J.N., Amuda A.K., Edmond R.R.D., Faisal M., Yusuf Y.D., 2021. Mapping of hydrothermal alterations related to gold mineralization within parts of the Malumfashi schist belt, North-Western Nigeria, *The Egyptian Journal of Remote Sensing and Space Science* 24(3): 401–417.

Baldridge A.M., Hook S.J., Grove C.I., Rivera G., 2009. The ASTER spectral library version 2.0. *Remote Sensing of Environment* 113(4): 711–715.

Baptista G.M.M., Corrêa R.S., dos Santos P.F., Madeira Netto J.S., Meneses P.R., 2011. Use of imaging spectroscopy for mapping and quantifying the weathering degree of tropical soils in Central Brazil. *Applied and Environmental Soil Science* 641328. DOI 10.1155/2011/641328.

Bedini E., 2009. Mapping lithology of the Sarfartoq carbonatite complex, southern West Greenland, using HyMap imaging spectrometer data. *Remote Sensing of Environment* 113(6): 1208–1219.

Chang C., Lin F., Zhou X., Zhao G., 2020. Hyper-spectral response and estimation model of soil degradation in Kenli County, the Yellow River Delta. *PLoS One* 15(1): e0227594.

Clark R.N., 1993. *SPECtrum Processing Routines user's manual version 3 (program SPECPR) (No. 93-595)*. US Geological Survey, Reston.

Clark R.N., 1999. Spectroscopy of rocks and minerals, and principles of spectroscopy. *Manual of Remote Sensing* 3(11): 3–58.

Clark R.N., King T.V., Klejwa M., Swayze G.A., Vergo N., 1990. High spectral resolution reflectance spectroscopy of minerals. *Journal of Geophysical Research: Solid Earth* 95(B8): 12653–12680.

Clark R.N., Roush T.L., 1984. Reflectance spectroscopy: Quantitative analysis techniques for remote sensing applications. *Journal of Geophysical Research: Solid Earth* 89(B7): 6329–6340.

Clark R.N., Swayze G.A., Gallagher A., King T.V.V., Calvin W.M., 1993. The U.S. Geological Survey digital spectral library, version 1: 0.2 to 3.0 um. *U.S. Geological Survey Open-File Report* 93–592.

de Jong S.M., 1994. *Applications of reflective remote sensing for land degradation studies in a Mediterranean environment.* The Royal Dutch Geographical Society, Utrecht University.

Demattê J.A.M., Garcia G.J., 1999. Alteration of soil properties through a weathering sequence as evaluated by spectral reflectance. *Soil Science Society of America Journal* 63(2): 327–342.

El-Desoky H.M., Tende A.W., Abdel-Rahman A.M., Ene A., Awad H.A., Fahmy W., El-Awny H., Zakaly H.M.H., 2022. Hydrothermal alteration mapping using landsat 8 and ASTER data and geochemical characteristics of Precambrian rocks in the Egyptian shield: A Case Study from Abu Ghalaga, Southeastern Desert, Egypt. *Remote Sensing* 14(14): 3456.

Gaffey M.J., 1976. Spectral reflectance characteristics of the meteorite classe. *Journal of Geophysical Research* 81(5): 905–920.

Goetz A.F., Srivastava V.I.N.A.Y., 1985. Mineralogical mapping in the Cuprite mining district, Nevada. In: *Proceedings of the airborne imaging spectrometer data analysis Workshop*. NASA Jet Propulsion Laboratory, California Institute of Technology, Pasadena, April 8–10, 1985.

Goetz A.F., Vane G., Solomon J.E., Rock B.N., 1985. Imaging spectrometry for earth remote sensing. S*cience* 228(4704): 1147–1153.

Grove C.I., Hook S.J., Paylorll E.D., 1992. *Compilation of laboratory reflectance spectra of 160 minerals, 0.4 to 2.5 micrometers*. NASA Jet Propulsion Laboratory, California Institute of Technology, Pasadena.

Gupta R.P., 2018. Geobotanical guides. In: Gupta R.P. (ed) *Remote Sensing Geology*. 3rdEdn. Springer-Verlag, Berlin: 347–348.

Heincke B., Jackisch R., Saartenoja A., Salmirinne H., Rapp S., Zimmermann R., Pirttijärvi M., Vest Sörensen E., Gloaguen R., Ek L., Bergström J., Karinen A., Salehi S., Middleton M., 2019. Developing multi-sensor drones for geological mapping and mineral exploration: Setup and first results from the MULSEDRO project. *Geological Survey of Denmark and Greenland Bulletin* 43: e20194303302.

Hellman M.J., Ramsey M.S., 2004. Analysis of hot springs and associated deposits in YellowstoneNational Park using ASTER and AVIRIS remote sensing. *Journal of Volcanology and Geothermal Research* 135: 195–219.

Hunt G.R., 1970. Visible and near-infrared spectra of minerals and rocks: I silicate minerals. *Modern Geology* 1: 283–300.

Hunt G.R., 1977. Spectral signatures of particulate minerals in the visible and near-infrared. *Geophysics* 42(3): 501–513.

Hunt G.R., Salisbury J.W., 1971. Visible and near infra-red spectra of minerals and rocks, II – Carbonates. *Modern Geology* 2: 23–30.

Hunt G.R., Salisbury J.W., Lenhoff C.J., 1971a. Visible and near infrared spectra of minerals and rocks, III – Oxides and hydroxides. *Modern Geology* 2: 195–205.

Hunt G.R., Salisbury J.W., Lenhoff C.J., 1971b. Visible and near infrared spectra of minerals and rocks, IV – Sulphides and sulphates. *Modern Geology* 3: 1–14.

Hunt G.R., Salisbury J.W., Lenhoff C.J., 1972. Visible and near infrared spectra of minerals and rocks, V – Halides, arsenates, vanadates, and borates. *Modern Geology* 3: 121–132.

Hunt G.R., Salisbury J.W., Lenhoff C.J., 1973. Visible and near infrared spectra of minerals and rocks, VI – Additional silicates. *Modern Geology* 4: 85–106.

Johnson J.R., Lucey P.G., Horton K.A., Winter E.M., 1998. Infrared measurements of pristine and disturbed soils 1. Spectral contrast differences between field and laboratory data. *Remote Sensing of Environments* 64: 34–46.

Kokaly R.F., Clark R.N., Swayze G.A., Livo K.E., Hoefen T.M., Pearson N.C., Wise R.A., Benzel W.M., Lowers H.A., Driscoll R.L., Klein A.J., 2017. USGS spectral library version 7. *U.S. Geological Survey Data Series* 1035.

Kortüm G., 1969. *Reflectance spectroscopy: Principles, methods, applications*. Springer Science & Business Media, Verlag New Your.

Kruse F.A., Lefkoff A.B., 1994. Knowledge-based geologic mapping with imaging spectrometers. *Remote Sensing Reviews* 8(1–3): 3–28.

Kumar C., Chatterjee S., Oommen T., Guha A., 2020. Automated lithological mapping by integrating spectral enhancement techniques and machine learning algorithms using AVIRIS-NG hyperspectral data in gold-bearing granite-greenstone rocks in Hutti, India. *International Journal of Applied Earth Observation and Geoinformation* 86: 102006.

Leone A.P., Sommer S., 2000. Multivariate analysis of laboratory spectra for the assessment of soil development and soil degradation in the southern Apennines (Italy). *Remote Sensing of Environment* 72(3): 346–359.

Liaghat S., Balasundram S.K., 2010. A review: The role of remote sensing in precision agriculture. *American Journal of Agricultural and Biological Sciences* 5(1): 50–55.

Martelet G., Gloaguen E., Døssing A., Silva E.L.S.D., Linde J., Rasmussen T.M., 2021. Airborne/UAV multisensor surveys enhance the geological mapping and 3D model of a pseudo-skarn deposit in Ploumanac'h, French Brittany. *Minerals* 11: 1259.

Michalski J.R., Kraft M.D., Sharp T.G., Christensen P.R., 2006. Effects of chemical weathering on infrared spectra of Columbia River Basalt and spectral interpretations of martian alteration. *Earth and Planetary Science Letters* 248(3–4): 822–829.

Mierczyk M., Zagajewski B., Jarocińska A., Knapik R., 2016. Assessment of imaging spectroscopy for rock identification in the Karkonosze Mountains, Poland. *Miscellanea Geographica* 20(1): 34–40.

Mohanty B., Gupta A., Das B.S., 2016. Estimation of weathering indices using spectral reflectance over visible to mid-infrared region. *Geoderma* 266: 111–119.

Mulder V.L., Plötze M., de Bruin S., Schaepman M.E., Mavris C., Kokaly R.F., Egli M., 2013. Quantifying mineral abundances of complex mixtures by coupling spectral deconvolution of SWIR spectra (2.1–2.4 μm) and regression tree analysis. *Geoderma* 207: 279–290.

Nagano T., Nakashima S., 1989. Study of colors and degrees of weathering of granitic by visible diffuse reflectance spectroscopy. *Geochemical Journal* 23: 75–83.

Pal M., Rasmussen T., Porwal A., 2020. Optimized lithological mapping from multispectral and hyperspectral remote sensing images using fused multi-classifiers. *Remote Sensing* 12(1): 177.

Parish R.M., 2016. Reflectance spectroscopy as a chert sourcing method. *Archaeologia Polona* 54: 115–128.

Park J., Kim K., 2019. Quantification of rock mass weathering using spectral imaging. *The Southern African Institute of Mining and Metallurgy* 119(12): 1039–1046.

Peyghambari S., Zhang Y., 2021. Hyperspectral remote sensing in lithological mapping, mineral exploration, and environmental geology: An updated review. *Journal of Applied Remote Sensing* 15(3): 031501.

Riaza A., Strobl P., Beisl U., Hausold A., Müller A., 1997. Spectral mapping of rock weathering degrees on granite using hyperspectral DAIS 7915 spectrometer data. *International Journal of Applied Earth Observation and Geoinformation* 3(4): 345–354.

Rockwell B.W., Hofstra A.H., 2008. Identification of quartz and carbonate minerals across northern Nevada using ASTER thermal infrared emissivity data – Implications for geologic mapping and mineral resource investigations in well-studied and frontier areas. *Geosphere* 4(1): 218–246.

Rogge D.M., Rivard B., Zhang J., Sanchez A., Harris J., Feng J., 2007. Integration of spatial–spectral information for the improved extraction of endmembers. *Remote Sensing of Environment* 110(3): 287–303.

Salehi S., 2018. Hyperspectral analysis of lithologies in the Arctic in areas with abundant lichen cover. *Geological Survey of Denmark and Greenland Bulletin* 41: 51–55.

Salehi S., Karami M., Fensholt R., 2016. Identification of a robust lichen index for the deconvolution of lichen and rock mixtures using pattern search algorithm (case study: Greenland). International archives of the photogrammetry. *Remote Sensing & Spatial Information Sciences* XLI-B7: 973–979.

Salehi S., Mielke C., Pedersen C.B., Olsen S.D., 2019. Comparison of ASTER and Sentinel-2 spaceborne datasets for geological mapping: A case study from North-East Greenland. *Geological Survey of Denmark and Greenland Bulletin* 43: e2019430205.

Salehi S., Mielke C., Rogass C., 2020. Mapping ultramafic complexes using airborne imaging spectroscopy and spaceborne data in Arctic regions with abundant lichen cover, a case study from the Niaqornarssuit complex in South West Greenland. *European Journal of Remote Sensing* 53(1): 156–175.

Salehi S., Rogge D., Rivard B., Heincke B.H., Fensholt R., 2017. Modeling and assessment of wavelength displacements of characteristic absorption features of common rock forming minerals encrusted by lichens. *Remote Sensing of Environment* 199: 78–92.

Salisbury J.W., Hunt G.R., 1974. Meteorite spectra and weathering. *Journal of Geophysical Research* 79(29): 4439–4441.

Schaefer L.N., Kereszturi G., Villeneuve M., Kennedy B., 2021. Determining physical and mechanical volcanic rock properties via reflectance spectroscopy. *Journal of Volcanology and Geothermal Research* 420: 107393.

Tong Q., Zheng L., Xue Y., 1998. Development and application of hyperspectral remote sensing in China. In: K.T. Tsen, H.R. Fetterman (eds.) *Proceedings of SPIE, the International Society for Optical Engineering,* San Jose, January 28 – 29, 1998

Traore M., Wambo J.D.T., Ndepete C.P., Tekin S., Pour A.B., Muslim A.M., 2020. Lithological and alteration mineral mapping for alluvial gold exploration in the south east of Birao area, Central African Republic using Landsat-8 operational land imager (OLI) data. *Journal of African Earth Sciences* 170: 103933.

Van der Meer F., Kopačková V., Koucká L., van der Werff H.M., Van Ruitenbeek F.J., Bakker W.H., 2018. Wavelength feature mapping as a proxy to mineral chemistry for investigating geologic systems: An example from the Rodalquilar epithermal system. *International Journal of Applied Earth Observation and Geoinformation* 64: 237–248.

Varshney P.K., Arora M.K., 2004. *Advanced image processing techniques for remotely sensed hyperspectral data*. Springer Science & Business Media, Berlin, Heidelberg: 38–39.

Xie B.S., Zhou S.Y., Wu L.X., 2020. An integrated mineral spectral library using shared data for hyperspectral remote sensing and geological mapping. *The International Archives of Photogrammetry, Remote Sensing and Spatial Information Sciences* 43: 69–75.

Younis M.T., Gilabert M.A., Melia J., Bastida J., 1997. Weathering process effects on spectral reflectance of rocks in a semi-arid environment. *International Journal of Remote Sensing* 18(16): 3361–3377.

Zhang X., Pazner M., Duke N., 2007. Lithologic and mineral information extraction for gold explorationusing ASTER data in the south Chocolate Mountains (California). *ISPRS Journal of Potogrammetry and Remote Sensing* 62(4): 271–282.

Zheng G., Ryu D., Jiao C., Xie X., Cui X., Shang G., 2019. Visible and near-infrared reflectance spectroscopy analysis of a coastal soil Chronosequence Guanghui. *Remote Sensing* 11: 2336.

Zhou K.F., Wang S.S., 2017. Spectral properties of weathered and fresh rock surfaces in the Xiemisitai metallogenic belt, NWXinjiang, China. *Open Geosciences* 9: 322–339.